August 24, 2001

Letter of Intent for a Linac Based PEP-N

Contributors:
M. Biagini, J. Clendenin, F.-J. Decker, D. Farkas, C. Pearson, J. Seeman, D. Sprehn, M. Sullivan, M. Woodley
Stanford Linear Accelerator Center, Menlo Park, CA 94025, USA
M. Placidi
CERN, Geneva, Switzerland
V. Azzolini
Ferrara University, Ferrara, Italy

I. Abstract

A new collider PEP-N is proposed to operate parasitically with the PEP-II collider at SLAC. This collider can operate in the energy range of the ϕ to the J/ψ using the positron beam of the PEP-II LER ring colliding with an electron beam from a newly constructed linac. The linac is copper based using SLAC spare linac sections pulsing at 120 Hz. The linac beam must be tunable in energy from 50 MeV to 800 MeV to cover the required center-of-mass energy range. The expected luminosity is above $10^{30}/cm^2/s$ between linac energies of 200 MeV and 700 MeV peaking at above $2.5x10^{30}$ at 350 MeV.

II. Introduction

A linac based collider for PEP-N was looked at several years ago [1] but was determined to be costly if continuous (cw) operation was considered. Also, a storage ring based collider was successfully studied [2]. However, recently at Snowmass 2001, pulsed operation was considered using SLAC linac specifications as used for the SLC. The resulting accelerator gives a luminosity for PEP-N which is acceptable for the desired physics. This new PEP-N arrangement with a linac is simpler in general when compared to a storage ring arrangement and is considerably less expensive.

III. Accelerator layout

The PEP-N collider would be located in the PEP-II Region 12 hall (IR12). A layout is shown in Figure 1 and the parameters are listed in Table 1. A copper linac is installed in the PEP-II tunnel in the 12A adit area adjacent to the existing PEP-II RF HER cavities. The linac extends through the IR12 collider hall to the collision point located in the 12B area. The beam dump is located in the 12B area keeping the linac electron “dump shine” shielded from the IR hall external radiation monitors.

Table 1 - PEP-N parameters using a pulsed linac.

PEP-N Accelerator Parameter	Units	Linac	PEP-II LER
Beam energy	MeV	50 to 900	3100
Maximum bunch charge	e^-	2.4×10^{10}	10^{11}
Bunch spacing	nsec	4.2	4.2
Pulses per second	Hz	120	Continuous
RF pulse length (flat top)	μsec	3.5	Continuous
Beam pulse length	μsec	3.8	----
Beam pulse length within 3% ΔE/E	μsec	3.5	----
Bunches per pulse		830	Continuous
Maximum linac current during pulse	mA	910	----
Invariant beam emittance	μm-rad	80	----
Beam energy spread	%	0.5	0.07
Klystron pulse power	MW	62	----
Klystron average power	kW	37	----
Total klystron power	kW	333	----
Maximum beam power (@400 MeV)	kW	140	----
Number of klystrons		9	----
Number of 3-m sections per klystron		2	----
Accelerating gradient	MeV/m	16.7	----
Acceleration per klystron	MeV	100	----
Gun pulse to pulse current jitter	%	2	----

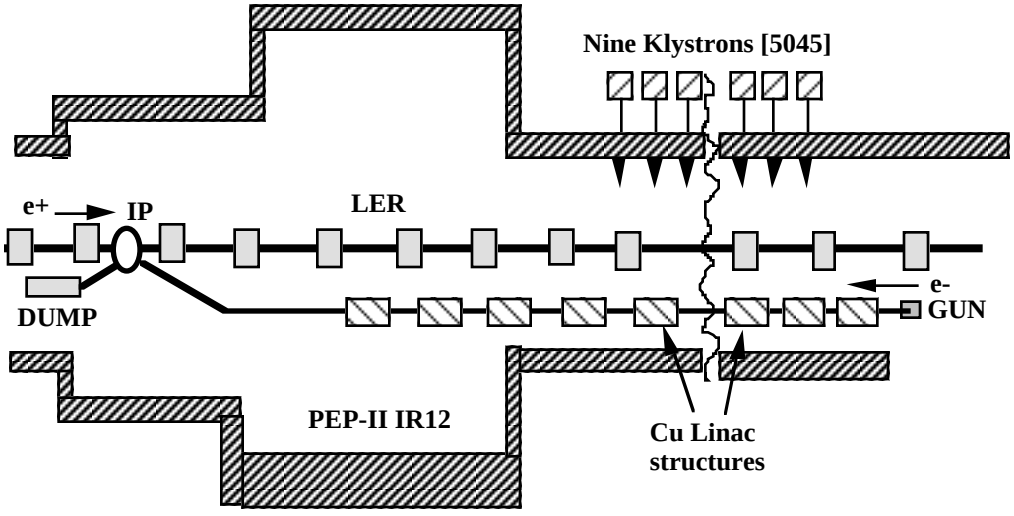

Fig. 1: Layout of PEP-II IR12.

IV. Collision parameters and layout

The linac electron bunches collide with the PEP-II LER positron bunches in the 12B area of the PEP-II tunnel. The linac operates in the long pulse mode with 830 bunches accelerated in the 3.5 μsec long pulse. To make a reasonable luminosity as the collision frequency is low, the spot sizes at the collision point must be as small as possible for both beams. The collision parameters are listed in Table 2 and a layout of the interaction region is shown in Fig. 2.

Since the PEP-II ring has 1660 colliding bunches, the linac will be timed to alternatively collide with the front or back 830 bunches each pulse.

Table 2 - PEP-N parameters at the interaction point at a linac energy of 350 MeV.

Parameter	Units	Linac	PEP-II LER
Energy	MeV	350	3100
Particle type		e^-	e^+
Pulse rate	Hz	120	Continuous
Colliding bunches per pulse		830	830
Bunch spacing	nsec	4.2	4.2
Bunch charge		2.4×10^{10}	10^{11}
IP energy acceptance	%	±3	---
Crossing angle	mrad	0.	0.
IP β_x	m	0.012	0.2
IP β_y	m	0.003	0.06
Bunch length	mm	3	11
Horizontal emittance ε_x	nm	117	25
Vertical emittance ε_y	nm	117	1
IP horizontal beam size	μm	37	71
IP vertical beam size	μm	19	8
IR betatron collimation	$\sigma_{x,y}$	2.5	15
Horizontal beam-beam tune shift	single pass	0.2	0.17
Vertical beam-beam tune shift	single pass	0.4	0.1
IP dipole length (including fringe field)	m	1.75	1.75
IP dipole field	T	0.3	0.3
Longitudinal polarization	%	80	0
Luminosity	$x10^{30}/cm^2/s$	2.5	2.5

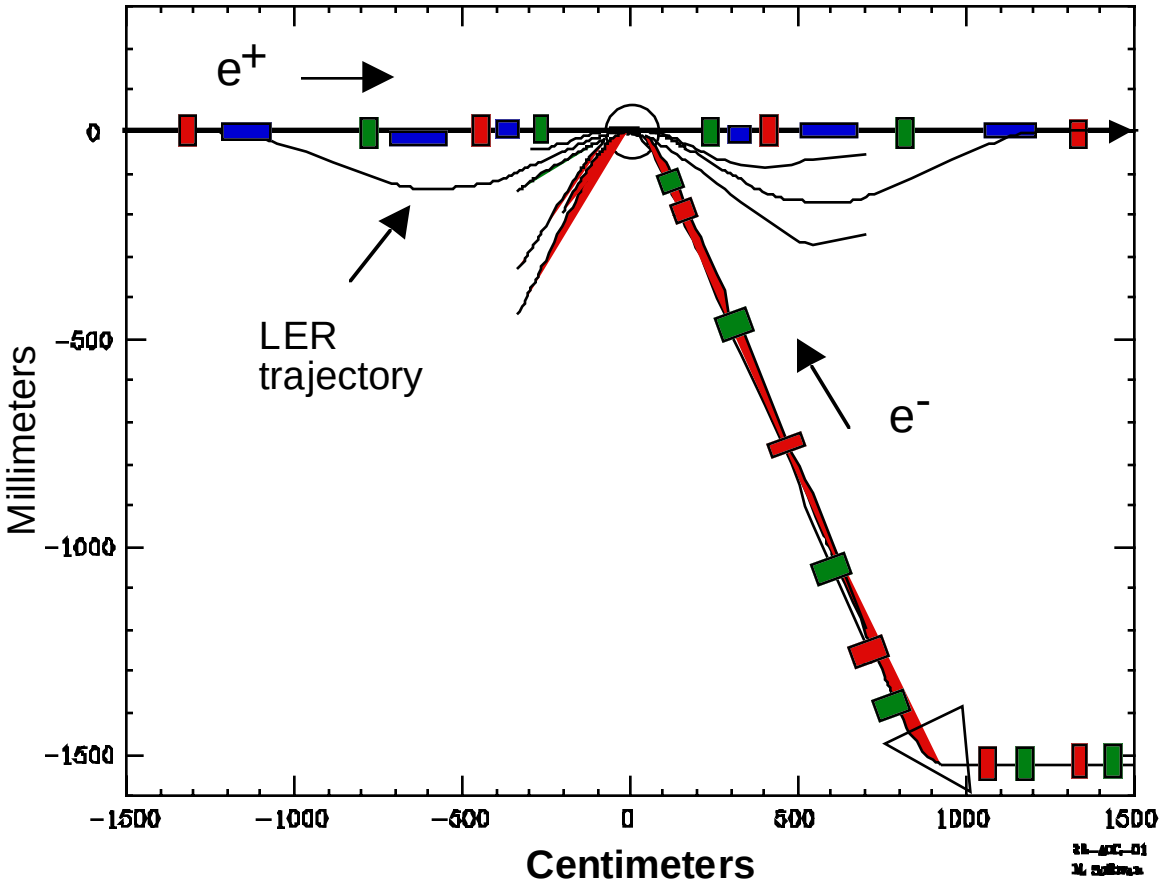

Fig. 2: Layout of PEP-N Interaction Region.

The luminosity will vary with the linac energy. The linac emittance is adiabatically reduced with acceleration leading to a higher luminosity at higher energy. However, the beam current loads the accelerator at high beam energy reducing the maximum current [3,4]. Furthermore, at low energy the gun charge jitter translates into energy jitter which is limited by the final focus optics. Thus, the maximum charge per bunch that can be accelerated in the linac is about 2.4×10^{10} e^-/bunch at 350 MeV but is linearly reduced to zero away from 350 MeV, as shown in Fig. 3. As a result, the luminosity is highest in the middle of the energy range, as shown in Fig. 4. The linac beam is collimated to ±4% in energy with the expectation that ±3% will collide. Betatron collimation will cut the beam at 2.5 $\sigma_{x,y}$ with the IP quadrupoles designed with 3 $\sigma_{x,y}$ clearance, all at 80 MeV linac energy. Higher energy beams pass more easily. The single pass beam-beam tune shifts were calculated as a function of the linac energy and are shown in Fig. 5. They are acceptable, taking into account that each LER bunch will have a collision in PEP-N every 2270 turns and the single pass values are only a few times the present PEP-II values. The LER damping time is about 7600 turns. The high linac tune shifts are acceptable for a single pass, as the bunches are discarded.

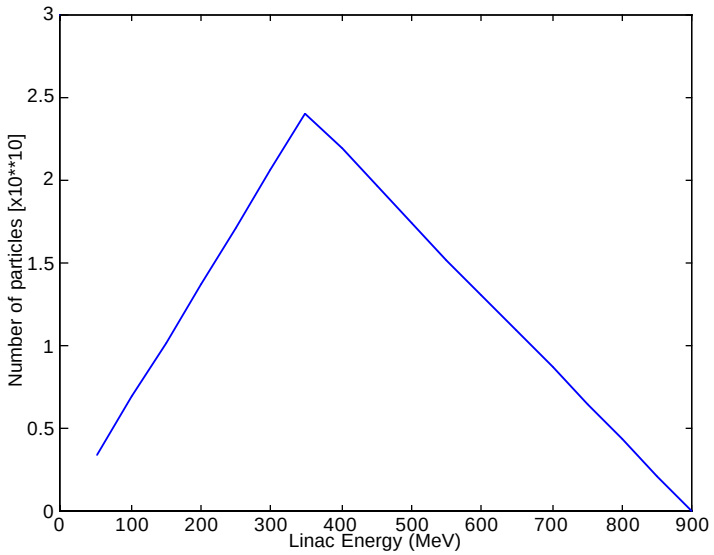

Figure 3 - Accelerated linac bunch charge versus energy.

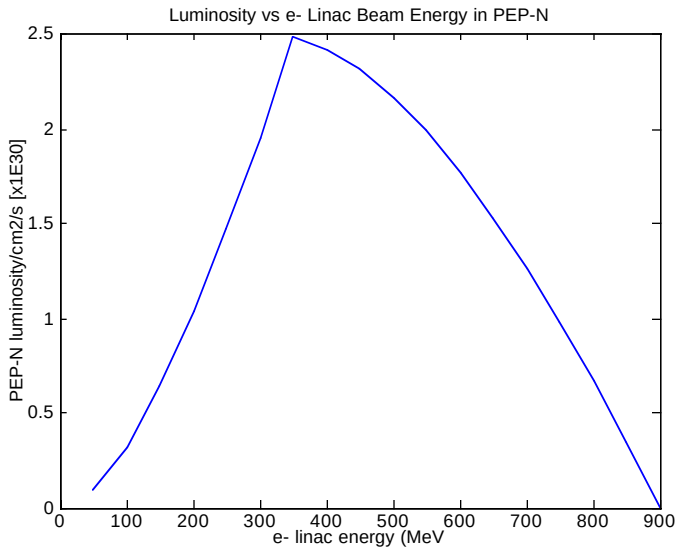

Fig. 4: PEP-N luminosity versus linac energy.

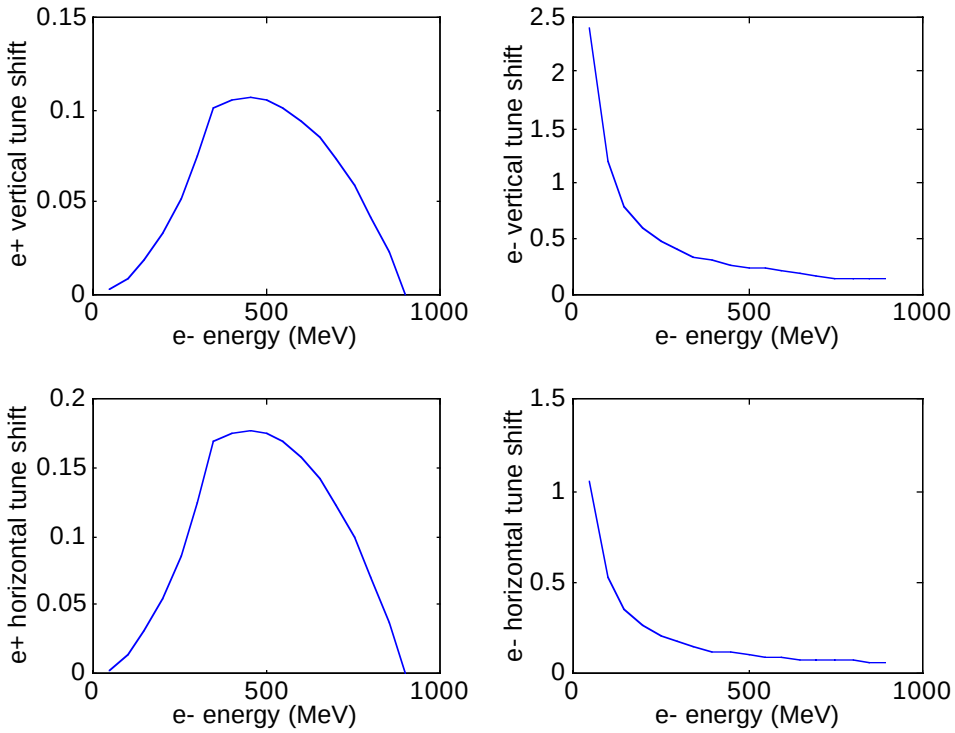

Fig. 5: Single pass beam-beam tune shifts versus linac energy. LER on the right side, Linac on the left. The e^+ single pass tune shifts should be divided by 2270 to get the average tune shift.

V. Electron gun

The electron gun must produce a string of about 900 bunches spaced 4.2 nsec apart each with a maximu charge of 2.4×10^{10} electrons at a repetition rate of 120 Hz. The gun will likely be a copy of the existing SLC laser gun with a photo-cathode emitter producing a polarization of about 80%. Additional energy capacity must be added to the gun to make the long train. There will be buncher cavities to longitudinally shape the train of bunches to a length of about 3 mm. Since a low transverse emittance is very important for this collider to make high luminosity, an output invariant emittance from the gun and linac of about 8×10^{-5} rad-m is desired.

The gun for polarized electrons will be the dc-biased SLAC polarized electron gun (PES) using the same type of HVPS as the SLAC thermionic gun. The desired bunch structure is not unlike that required for the NLC except the macropulse is longer, resulting in higher total charge. With a cw laser, the dc-biased polarized gun will produce an electron bunch identical to that from the thermionic gun, except it will be polarized. Thus subharmonic and S-band bunchers will still be required and an efficiency of only 50% is assumed. The capacitance of the SLAC polarized gun should be ~170 pF, corresponding to a stored energy of ~2 J. Another joule is stored in the HV cable. The beam loading will be

6%. The laser power is important. J_{MB}^{Cath} is the laser energy at the excitation wavelength delivered to the cathode:

$$J_{MB}^{Cath} = \frac{n_e hc}{\lambda QE} = \frac{2x10^{-25} n_e}{\lambda}$$

where *QE* is the quantum efficiency of the cathode at the excitation wavelength, λ. Excitation at 850 nm assumes a thin GaAs crystal for high polarization, thus the *QE* is quite low. A laser pulse with microstructure cannot be used with a dc-biased gun because of space charge effects in the electron beam, i.e., the energy of the beam is too low for too long. Note that for SLC the typical gun pulse was $8x10^{10}$ e^- in 2 ns or a current density of i_{pk}=20 A cm^{-2}, whereas here the requirement is $2x10^{10}$ e^- in 100 ps or i_{pk}=100 A cm^{-2}. (A fully illuminated cathode of radius 1 cm is assumed in both cases.) Thus the laser pulse should be dc during the macropulse (dc MP), meaning no micropulse structure.

VI. Linac

The linac will consist of nine girders using two existing ten-foot SLAC accelerating sections followed by a quadrupole double, a BPM, and a pair of corrector magnets. Each girder will be powered by an existing K5045 SLC klystron with a flat top pulse length of 3.5 μsec and a power of 62 MW. The accelerating gradient will be about 17 MeV/m for a total acceleration of 100 MeV for each girder. Nine girders will give 900 MeV of beam energy not taking into account beam loading.

A schematic drawing of a linac girder is shown in Fig. 6. The lattice for the linac up to last accelerating structure is shown in Fig. 7. The resulting beam sizes with an invariant emittance of $8x10^{-5}$ rad-m, are shown in Fig. 8.

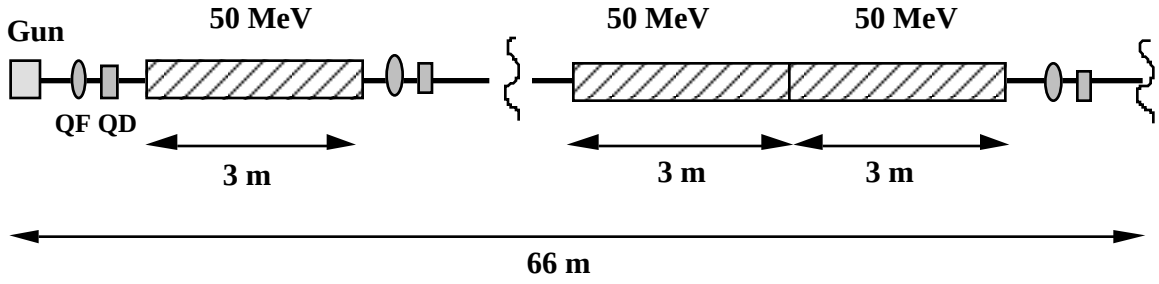

Fig. 6: Layout of linac structures.

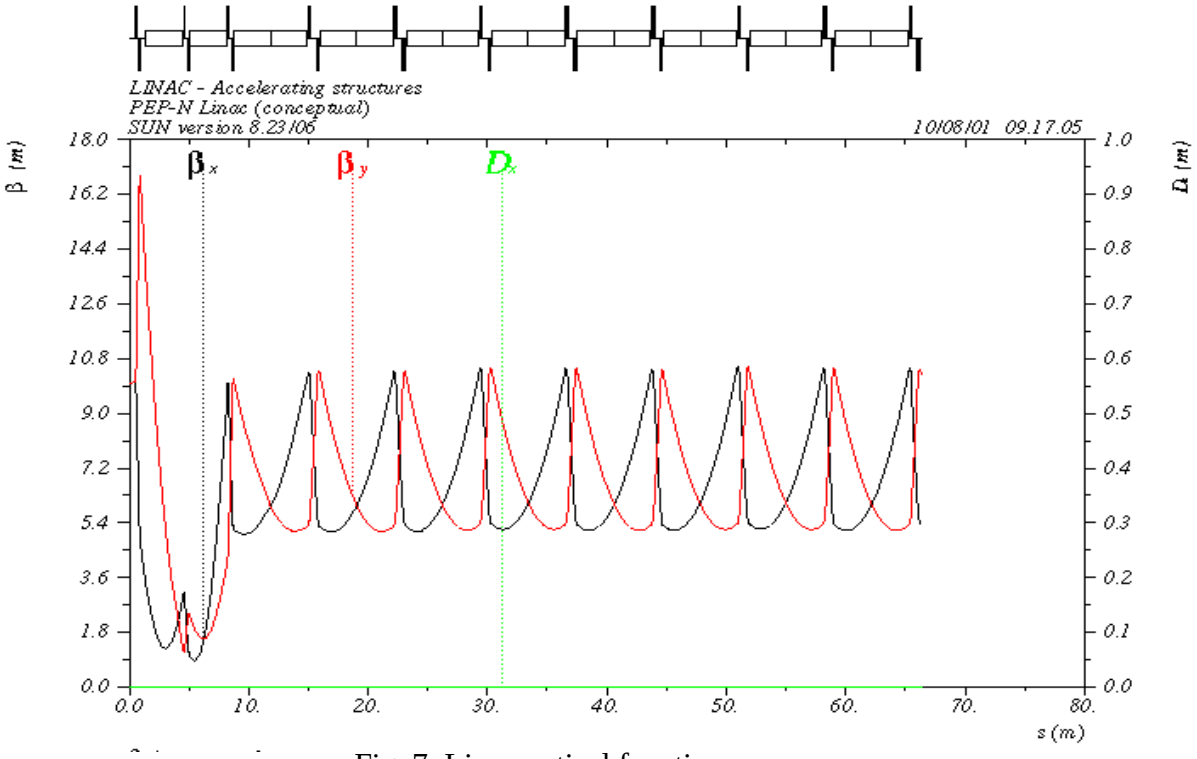

Fig. 7: Linac optical functions.

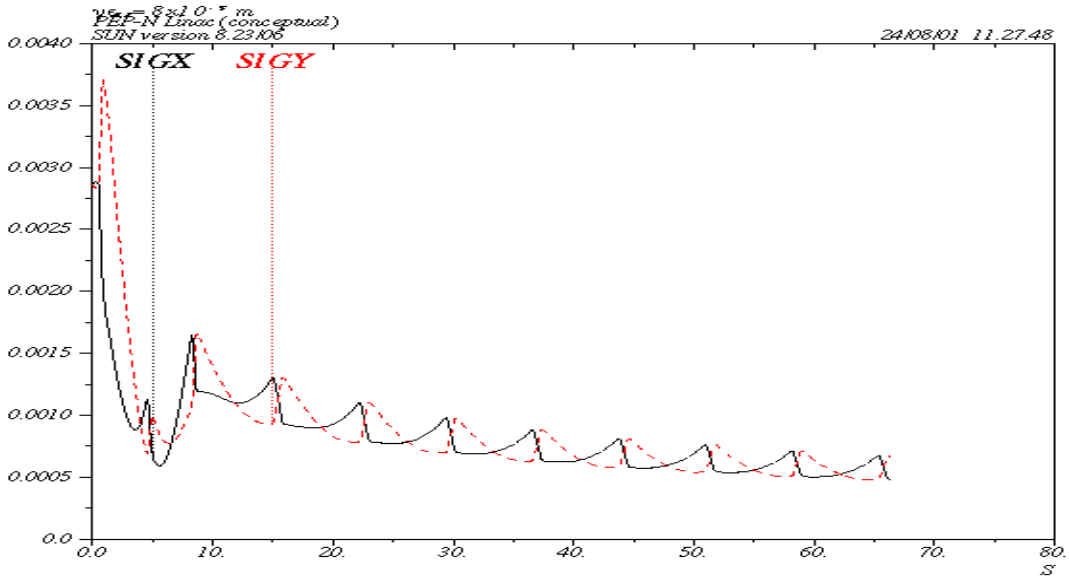

Fig. 8: Linac beam sizes for $8x10^{-5}$ m-rad emittance (in meters).

The linac quadrupoles are existing QA and QB magnets removed from the linac and presently unused. These magnets use 8 A of current at less than 30 Volts which is a convenient corrector power supply at SLAC. There are several extra quadrupoles early in the linac to reduce wakefield effects. Four quadrupoles (QC) between the end of the linac

section and the first bending magnet will provide the matching of the optical functions to the IP. The quadrupole strengths are listed in Table 3.

Table 3 - Linac magnet parameters

Linac magnet parameter	Units	Value
Quad QA length	m	0.102
Quad QA max gradient @ 100 MeV	T/m	5.5
Quad QB length	m	0.202
Quad QB max gradient @ 900 MeV	T/m	8.5
Quad QC length	m	0.4
Quadr QC max gradient @ 800 MeV	T/m	13.6

The klystrons can be powered by existing modulators located in Sector 20 of the linac which are not needed for PEP-II or the LCLS. The SLED cavities are not used. The average power of each klystron is about 37 KW resulting in a total power of about 350 kW which is available in Region 12. Heaters will be provided to keep the accelerator at 113° F when the linac is not pulsing.

The beam charge loads the RF of the linac and must be compensated near the leading edge of the pulse. A simulation of this is shown in Fig. 9. The upper curve is the combined RF pulse without loading. The beam is injected when the cavities are filled, in the next curve. Injecting the beam on the rising slope with a 3.5 us long pulse and the same charge gives a smaller energy variation during the 825 ns fill time. The bottom two curves show a longer pulse if the beam pulse is further lengthened. The 3.8 μsec curve (red) is the one used in the design..

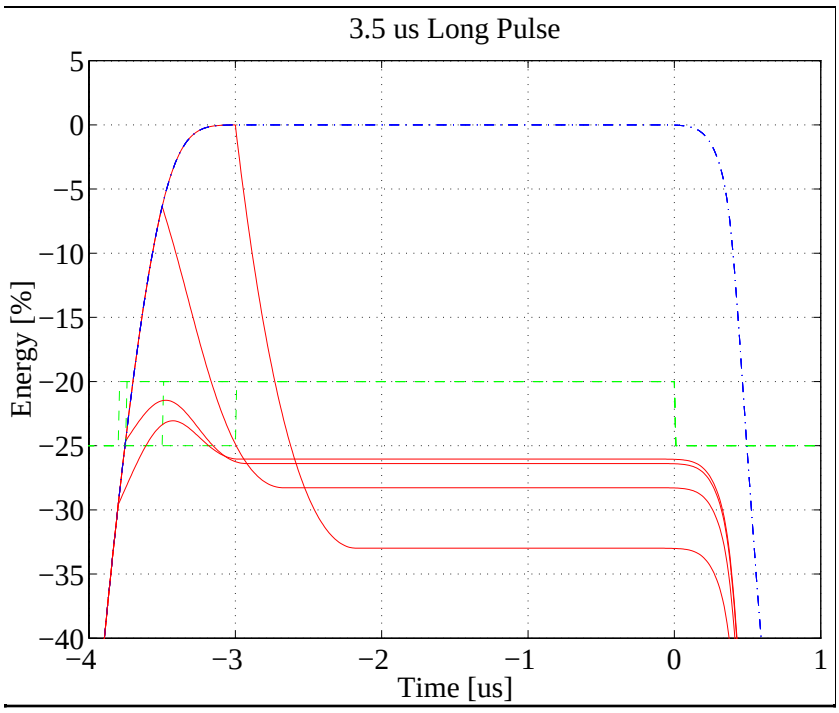

Fig. 9: Beam loading of a 3.0 and 3.5 μsec long pulse containing $7x10^{12}$ particles.

VII. Linac to Interaction Point

The magnetic layout of the transfer line from the linac end to the IP is shown in Fig. 10. The optical functions are shown in Fig. 11. The detector magnetic field will be used to provide the beam separation needed before and after the IP. The transfer line will then consist of a bending magnet (BL) with the same parameters as the detector dipole and a quadrupole arrangement such as to provide both the focusing and the needed dipersion control.

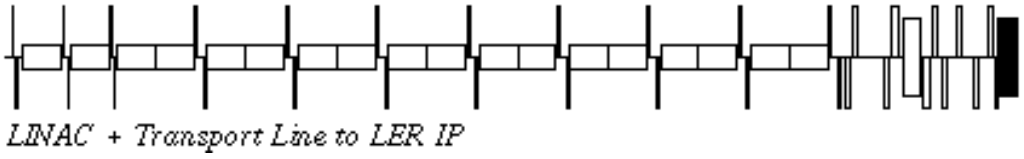

Fig. 10: Linac + Final Focus lattice (80 m length).

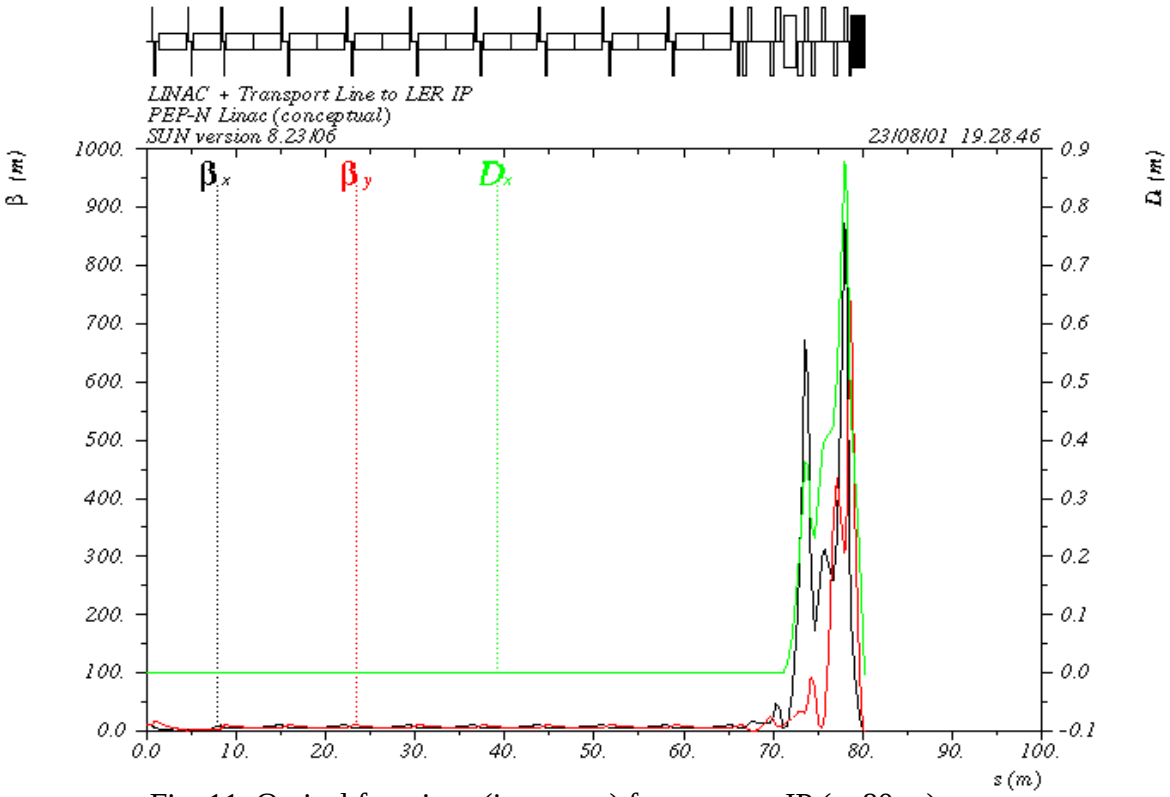

Fig. 11: Optical functions (in meters) from gun to IP (at 80 m).

In an achromatic 'dog-leg' a QD-QF doublet is used to focus the beam at the IP where β_x is 12 mm and β_y is 3 mm. At the IP the horizontal dispersion η_x is matched to zero, but its derivative, η_x', is 0.5 rad. The first IP quadrupole, located at 1.5 m from the IP, would be permanent magnet in order to leave as much space as possible for the detector components. The detector dipole (B0) field is bell-shaped to take into account the fringe fields. Five quadrupoles in this section plus four at the linac accelerating structure end, before the BL dipole, will match dispersion and beta functions to the linac values. Table 4 lists the magnetic parameters of this section for an 800 MeV beam. The optical functions

from the IP to the BL dipole are shown in detail in Fig. 12. The beam sizes at 800 MeV are plotted in Fig. 13 for the whole structure.

The linac beam after passing through the collision point is allowed to grow naturally and then is deposited into a dump. An existing dump from the SLAC Beam Switch Yard of the required capacity is available.

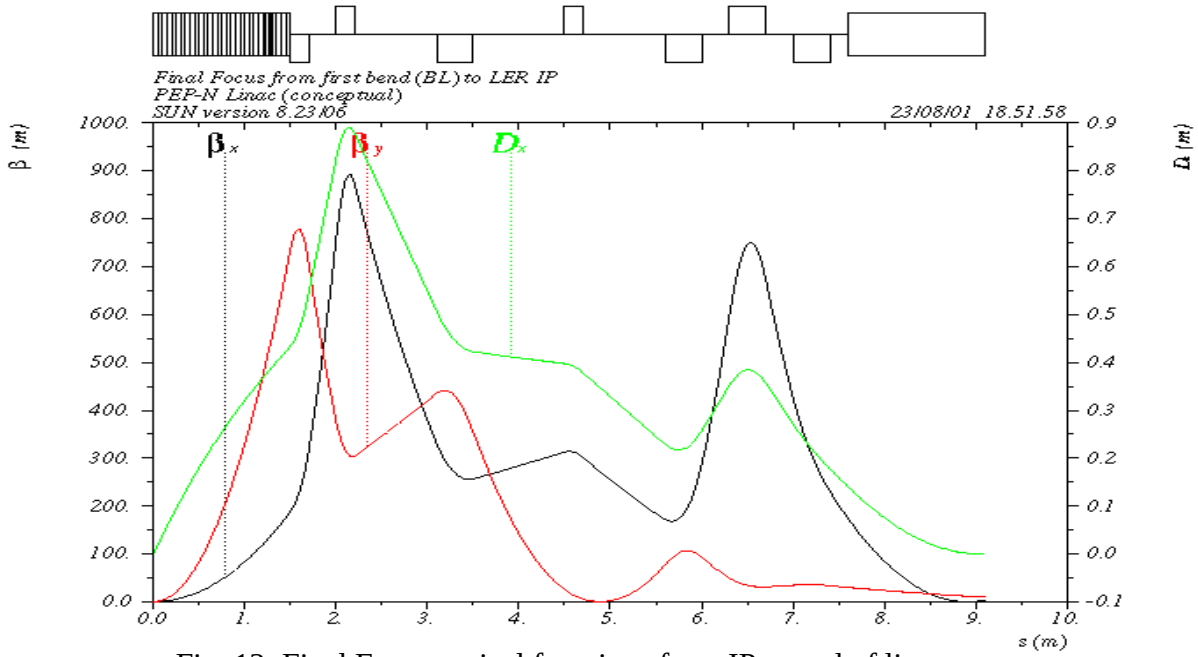

Fig. 12: Final Focus optical functions from IP to end of linac.
The 'downstream' detector dipole is shadowed.

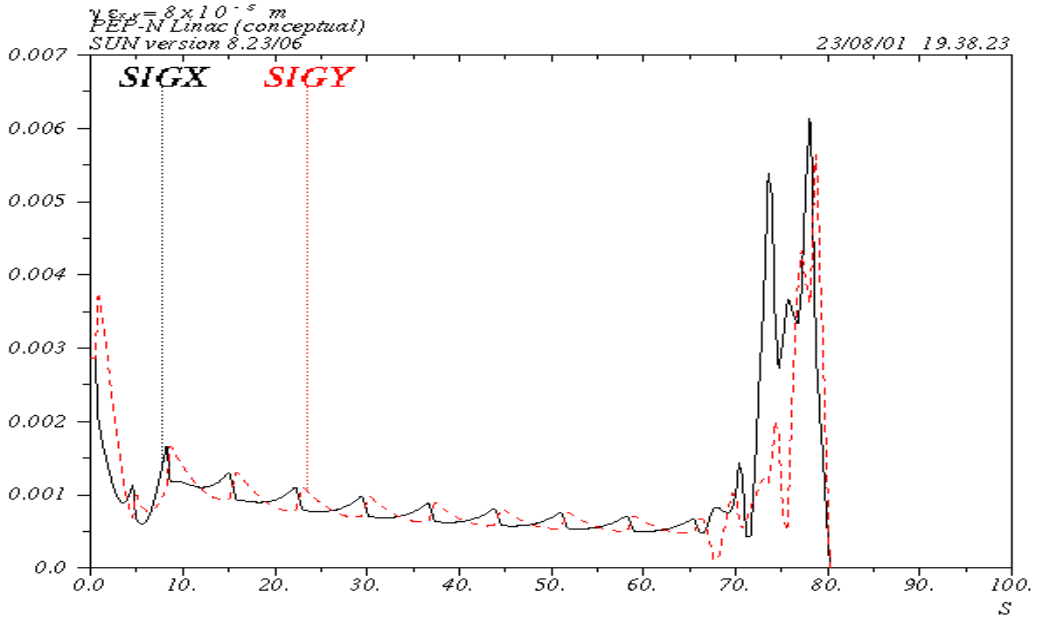

Fig.13: Beam sizes at 800 MeV (in meters) from gun to IP (at 80 m).

Table 4 - Linac to IP magnet parameters @ 800 MeV

Magnet parameter	Units	Value
Matching linac quads length	m	0.4
Matching linac quads max gradient	T/m	16.
First linac dipole (BL) length	m	1.5
First linac dipole (BL) field	T	0.4
First linac dipole (BL) bending angle	rad	0.192
Matching doublet quads length	m	0.4
Matching doublet quads max gradient	T/m	11.
Central focusing quad length	m	0.2
Central focusing quad max gradient	T/m	9.
Central defocusing quads length	m	0.4
Central defocusing quad max gradient	T/m	10.
IP doublet quads length	m	0.2
IP quads max gradient	T/m	21.
Detector dipole (B0) length downstream IP	m	1.5
Detector dipole (B0) field	T	0.42
Detector dipole (B0) angle (fringe field included)	rad	0.192

VIII. Interaction Region

The interaction region is basically the same as that used in the storage ring design. The central dipole field is shifted 25 cm downstream in order to improve the detector acceptance and, at the same time, minimize the upstream bending in the LER. The beam from the LINAC passes through a final focus doublet with the last magnet before the IP located 1.5 m away. This magnet is made from permanent magnet material in order to keep the magnet dimensions small and compact and to maximize the forward angle acceptance of the detector.

After the LINAC beam passes through the collision point it is allowed to naturally blow up by not having any focusing elements in the beam line until about 3 m from the IP. This spreads out the beam power making it easier to absorb this power in the dump. The beam separation at the first LER quad (2.6 m from the IP) is about 20 cm. This is twice the separation PEP-II has for QF2, a similar magnet located 2.8 m from the PEP-II IP. The separation implies the need for a special LER quad at this location, however, the greater beam separation means that this quad will be significantly easier to build than the one used in PEP-II.

The central dipole field is held at a constant value of 0.3 T over a LINAC energy range of approx. 200-500 MeV. This is achieved by adding passive magnetic shielding to the beam pipes as the LINAC energy decreases. No magnetic elements need to be moved over this energy range. In order to reach a LINAC energy of 800 MeV the central field is increased to 0.42 T. So, for an energy range of about 200-800 MeV the central field has only two operating points.

Electron energies below 200 MeV have not been studied yet and it is likely that the electron beam lines will have to be repositioned to accommodate these lower beam energies while we keep the detector field at or near 0.3 T.

Detector backgrounds are dominated by the LER and the LER design is very much the same for both the storage ring and LINAC designs so detector backgrounds should be essentially the same. The only difference might be in that the luminosity per collision for the LINAC design is higher than for the ring design and therefore the background per unit

luminosity would be lower for the LINAC design. The detector dipole is shown in Fig. 14. The field map, shown in Fig. 15, is used to separate the beams before and after the collisions.

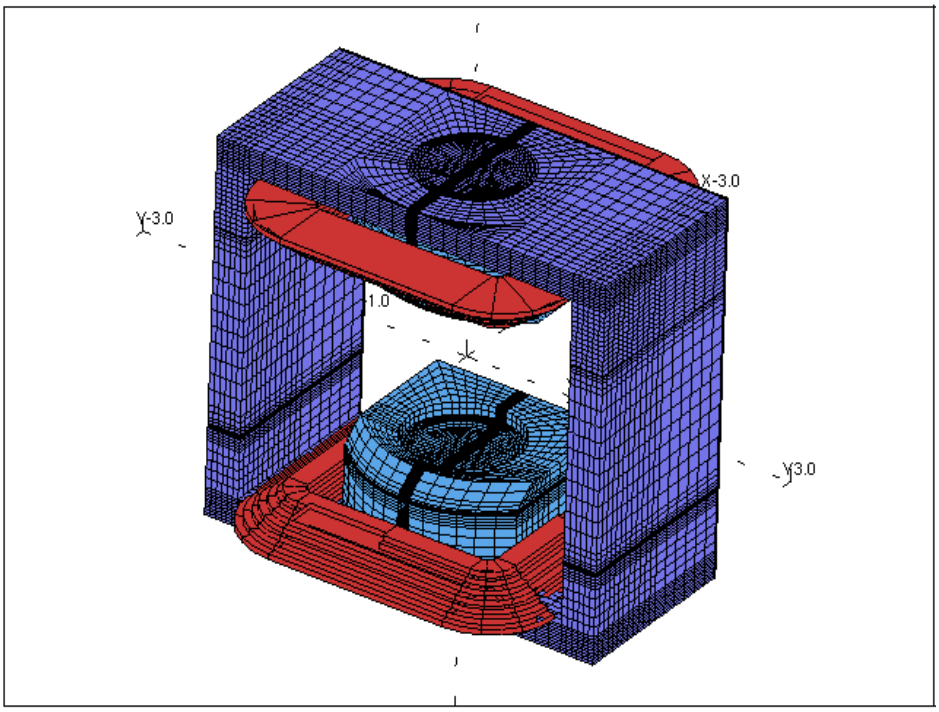

Fig. 14: Detector dipole.

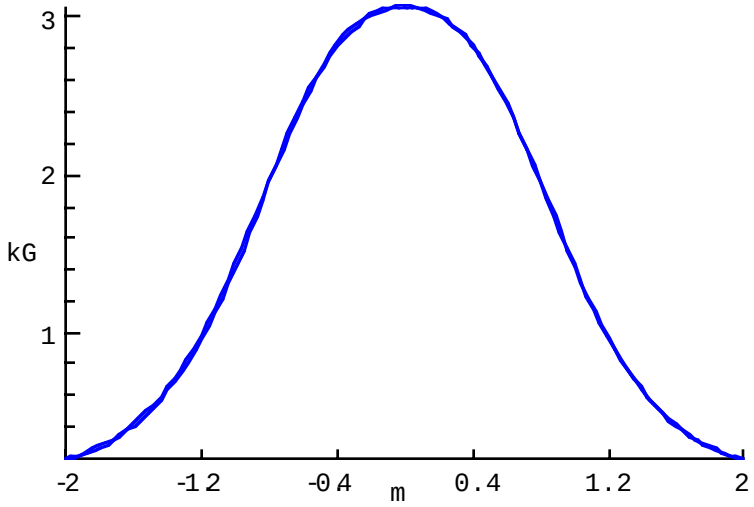

Fig. 15: Plot of the magnetic field from the central dipole magnet. The field extends out to at least 2 m from the center.

A sketch of the beam trajectory from the linac end to the IP and the dump is shown in Fig. 16. In Table 5 the geometric parameters for different energies are listed.

Table 5: Parameters for the linac Interaction Region (c =1.5 m, e=.25 m)

E^- /GeV	$\int B\,dl$ /T m	$\langle B \rangle$ /T	Shield	θ /rad	ρ /m	a /m	b /m
0.08	0.24	0.30	Y	0.900	0.889	1.62	1.915
0.30	0.36		N	0.360	3.333	4.59	4.258
0.50	0.40	0.42	Y	0.240	3.968	6.61	6.310
0.80	0.51		N	0.192	6.349	8.33	7.861

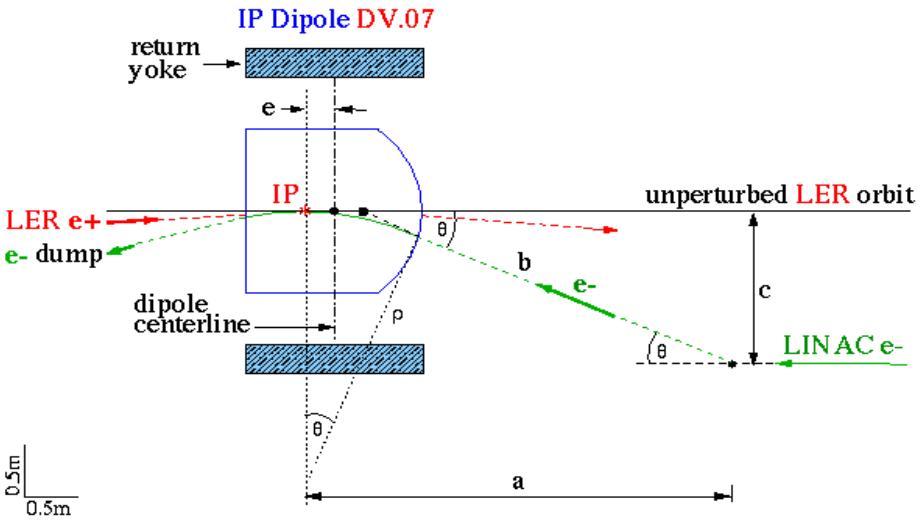

Fig. 16: Beam trajectory from linac to IP and dump.

The quadrupoles in the linac IR need a large bore to pass the beam. The bore is determined by 3 $\sigma_{x,y}$ and 3% energy offset. The resulting bore of the final focus doublet needs to be about 18 cm @ 80 MeV, 12 cm @ 350 MeV, and 10 cm @ 800 MeV. The larger bore is compensated by a lower energy. Thus, different quadrupoles can be used at different energies.

IX. LER lattice

The lattice in the LER needs to be modified to make a low beta insertion at the collision point of PEP-N. None of the existing quadrupoles will be moved. However, three quadrupoles and six dipole magnets must be added to make the low betas and to compensate for the dipole field at the collision point that separates the beams. The beta functions in the LER are shown in Fig. 17 and the resulting magnet strengths in Table 6. The optics is matched to the standard LER values at the end of this section. The standard LER quadrupoles are adequate for this new configuration.

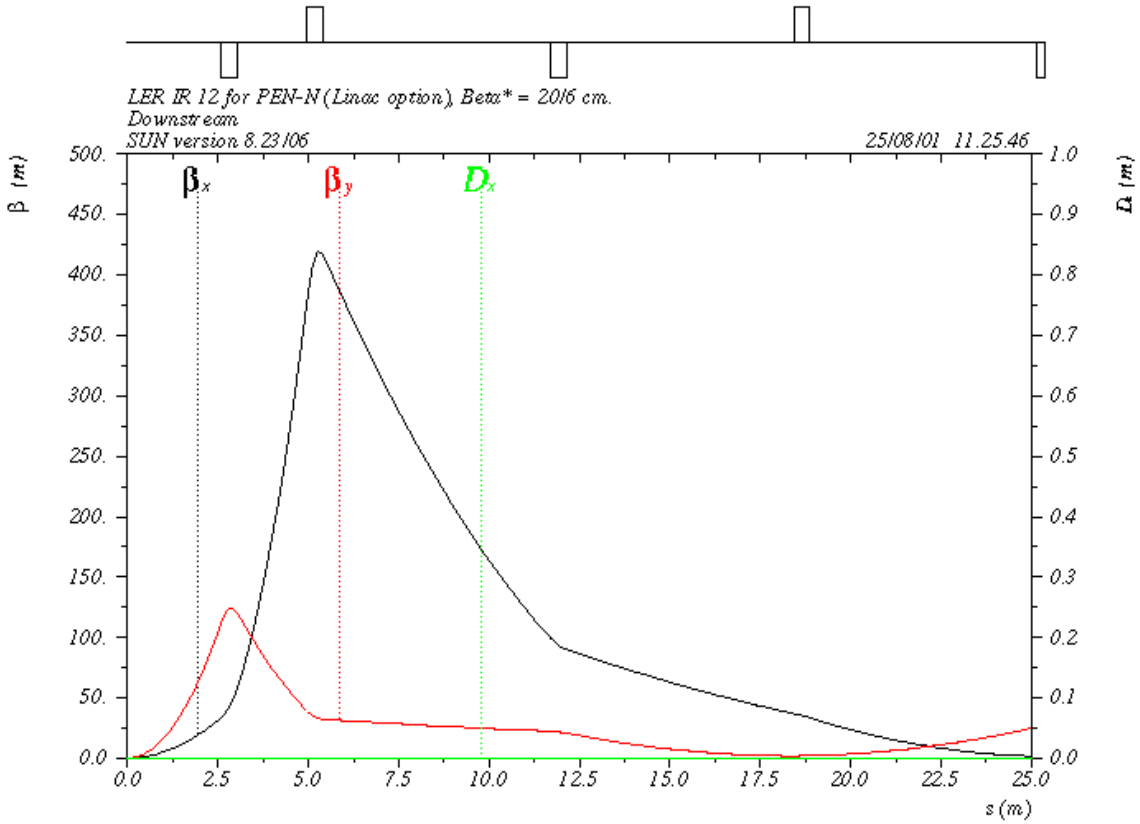

Fig. 17: LER IR optical functions from the IP to the midpoint of straight 12 (downstream the detector).

Table 6 - New LER IR magnet parameters

Magnet parameter	Units	Value
Focusing quad length	m	0.43
Focusing quad gradient	T/m	13.
Defocusing quad length	m	0.43
Defocusing quad gradient	T/m	7.

X. HER modifications

The HER in this configuration is not modified. The HER vacuum chamber passes through the pole of the IP dipole and is, thus, not directly affected. However, there is a small amount of fringing magnetic field upstream and downstream of the dipole that must be either shielded or corrected with small dipoles.

XI. Preliminary Costs and Schedules

The approximate costs of this accelerator have been estimated and are shown in Table 7. The following items have been assumed to be “borrowed” from the SLAC linac as they are unused now or are not needed for the LCLS program: 9 klystrons, 9 modulators, 9 RF controls, 18 accelerator section and loads, 16 QB quadrupoles, 8 QA quadrupoles, 30 corrector dipoles, and 18 position monitors.

The entire linac could be constructed in about one year and installed in a 3 month downtime, if funds and engineers are available.

Table 7 - Approximate cost of a linac based PEP-N

Accelerator Item	**Number of items**	**Cost (k$)**
Polarized gun	1	500
Linac girder	18	300
Linac klystrons, modulator, controls	9	500
Linac RF waveguide	9	300
Linac waveguide water and heaters	9	200
Linac near IR dipole	1	15
Linac IR quadrupoles	11	110
Linac vacuum system	20 m	200
Linac BPMs	16	65
Linac energy and energy spread monitor	1	20
Linac current monitor	1	15
Linac dump	1	30
Linac shielding	1	100
Linac AC power equipment	1	300
Linac PPS controls	1	100
Linac magnet power supplies	25	300
LER power supplies	7	350
LER vacuum chambers	4	300
LER quadrupoles	3	60
LER dipole	4	60
HER corrector dipoles	2	15
Installation	lot	360
Alignment	lot	50
Engineering	1 year	100
Drafting	2 years	150
Subtotal cost		**4500**
Contingency (30%)		1300
Indirects (30%)		1700
Total cost		**7500**

X. References

[1] P. Patteri, “A feasibility study of an asymmetric e+e- linac-ring collider at $\sqrt{s} \approx 2$ GeV with some existing storage rings”, LNF-99/031(IR), Frascati, Oct. 1999.

[2] “PEP-N Letter of Intent,” PEP-II AP Note: 2000.05, Sept. 2000.

[3] Z.D.Farkas, “Variable current transient beam loading compensation”, SLAC-AP-133, Oct. 2000.

[4] “SLAC LINAC BLUE BOOK”, R. Neal Editor, p.117, 1968.